

# Impulse wave generation: Comparison of free granular with mesh-packed slides

**Journal Article****Author(s):**

Evers, Frederic M.  Hager, Willi H.

**Publication date:**

2015-03

**Permanent link:**

<https://doi.org/10.3929/ethz-a-010814662>

**Rights / license:**

[Creative Commons Attribution 4.0 International](#)

**Originally published in:**

Journal of Marine Science and Engineering 3(1), <https://doi.org/10.3390/jmse3010100>

*Article*

## Impulse Wave Generation: Comparison of Free Granular with Mesh-Packed Slides

Frederic M. Evers \* and Willi H. Hager

Laboratory of Hydraulics, Hydrology and Glaciology (VAW), ETH Zurich, CH-8093 Zürich, Switzerland; E-Mail: hager@vaw.baug.ethz.ch

\* Author to whom correspondence should be addressed; E-Mail: evers@vaw.baug.ethz.ch; Tel.: +41-44-633-0877; Fax: +41-44-632-1192.

Academic Editor: Valentin Heller

*Received: 14 October 2014 / Accepted: 12 February 2015 / Published: 4 March 2015*

---

**Abstract:** Slides generating impulse waves are currently generated using either block models or free granular material impacting a water body. These procedures were mainly developed to study plane impulse waves, *i.e.*, wave generation in a rectangular channel. The current VAW, ETH Zurich, research is directed to the spatial impulse wave features, *i.e.*, waves propagating in a wave basin. The two wave generation mechanisms mentioned above complicate this process for various reasons, including experimental handling, collection of slide material in the wave basin, poor representation of prototype conditions for the block model, and excessive temporal duration for free granular slides. Impulse waves originating from slides with free granular material and mesh-packed slides are compared in this paper. Detailed test series are presented, so that the resulting main wave features can be compared. The results highlight whether the simplified procedure involving mesh-packed slides really applies in future research, and specify advantages in terms of impulse wave experimentation.

**Keywords:** hydraulics; impulse product parameter; impulse wave; physical modeling; subaerial landslide; water wave

---

## 1. Introduction

Mass wasting including rockfalls, landslides, or avalanches may cause large water waves in oceans, bays, lakes, and reservoirs. As the kinetic energy is transferred from the slide mass to the water body these waves are referred to as impulse waves. They may run-up the shoreline several meters or overtop a dam, endangering thereby adjacent settlements and infrastructure. Therefore, procedures for assessing the generation and propagation of landslide-generated impulse waves form the integral part of an effective risk management strategy [1].

The generation of landslide-generated impulse waves is a complex process encompassing the interaction of the phases slide material, water, and air. To reproduce this process within a hydraulic scale model subaerial slides have so far been mainly represented by either a free granular slide or a rigid block [2]. Free granular slide material was used e.g., by Fritz [3], Heller [4], Mohammed and Fritz [5], and Viroulet *et al.* [6]; while e.g., Di Risio *et al.* [7], Heller and Spinneken [2], Kamphuis and Bowering [8], Noda [9], Panizzo *et al.* [10], Sælevik *et al.* [11], and Viroulet *et al.* [12] conducted experiments with block models. Ataie-Ashtiani and Nik-Khah [13] and Zweifel [14] presented results comprising both approaches. Block models are unable to account for the granular slide matrix, whereas free granular slides imply a significant procedural and temporal effort for the experimental execution.

Fritz [3], Zweifel [14], and Heller [4] conducted a total of 434 experiments involving free granular material and a pneumatic landslide generator using the two-dimensional (2D) wave channel at the Laboratory of Hydraulics, Hydrology and Glaciology (VAW). The relevant wave characteristics were among others the maximum wave amplitude and wave height, as well as their decay along the propagation distance [4]. The observed wave characteristics were correlated to the measured slide parameters to establish general design information. These empirical equations for significant wave parameters are used as a reference for the experiments presented hereinafter, since they were established on a sound data basis.

As described by Slingerland and Voight [15], Davidson and Whalin [16] also applied bags containing loose iron and lead elements for generating impulse waves. Yet their results were not compared to free granular slides. As a prerequisite to investigate the generation and propagation of spatial impulse waves in a wave basin, experiments with mesh-packed granular material in a 2D wave channel were conducted. The focus of these tests comprised only selected wave features as the wave amplitudes and heights, their decay, and the wave crest celerity. However, no comprehensive test program involving further test parameters was attempted, because this will be the purpose of future research. The measured wave characteristics are compared with the empirical equations derived from the 2D data resulting from the free granular material to assess whether mesh-packed slides provide a sufficient reproducibility. The following therefore involves a comparison between free and mesh-packed slides to investigate whether the simplifications offered by the latter approach are justified by the experimental data. If mesh-packed slides would be able to adequately reproduce the former approach, substantial simplifications in terms of experimental effort, test duration including material package and collecting from the test facility, among others, would result.

## 2. Previous Research and Experimental Setup

### 2.1. Impulse Product Parameter

2D experiments involving free granular material were conducted by systematically varying the slide parameters to study 2D impulse waves. Heller and Hager [17] identified the slide (subscript *s*) impact velocity  $V_s$ , the slide thickness  $s$ , the slide mass  $m_s$ , the still water depth  $h$ , and the slide impact angle  $\alpha$  as the relevant parameters for impulse wave generation (Figure 1). A set of dimensionless quantities, namely the slide Froude number  $F$ , the relative slide thickness  $S$ , and the relative slide mass  $M$ , entirely define the physics of impulse waves, namely

$$F = V_s/(gh)^{1/2} \quad (1)$$

$$S = s/h \quad (2)$$

$$M = m_s/(\rho_w b h^2) \quad (3)$$

Based on these dimensionless quantities, Heller and Hager [17] developed the so-called impulse product parameter  $P$  for describing the 2D characteristics of landslide generated impulse waves as

$$P = FS^{1/2}M^{1/4}\{\cos[(6/7)\alpha]\}^{1/2} \quad (4)$$

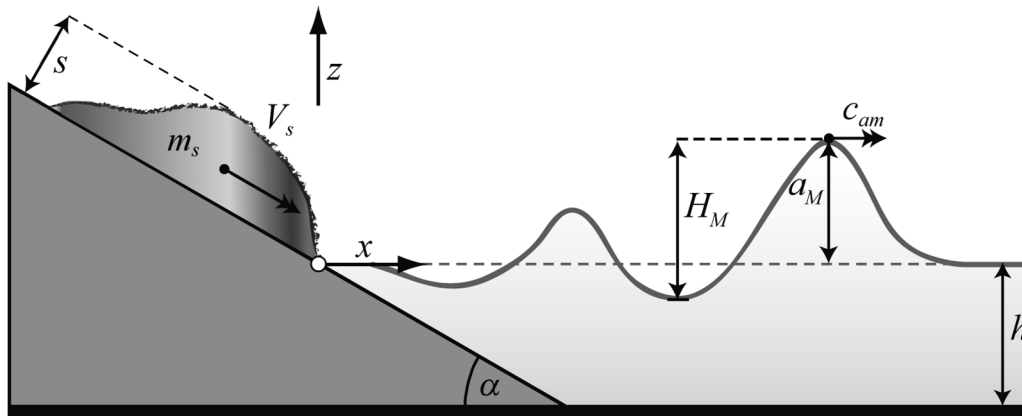


**Figure 1.** Relevant slide parameters and wave characteristics (adapted from Heller [4], with permission from VAW).

### 2.2. Wave Characteristics

To study the reproducibility of waves generated by mesh-packed slides compared with free granular slides, the maximum (subscript *M*) wave amplitude  $a_M$  and the maximum wave height  $H_M$  as shown in Figure 1, as well as their decay along the propagation distance  $x$  were analyzed. The governing 2D wave characteristics include the relative maximum wave amplitude  $A_M = a_M/h$  and height  $Y_M = H_M/h$  plus their decay  $A(X)$  and  $Y(X)$  along the relative distance  $X = x/h$  measured from the location of the free water surface at the slide plane (Figure 1). Heller and Hager [17] empirically derived these wave characteristics as

$$A_M = (4/9)P^{4/5} \quad (5)$$

$$Y_M = (5/9)P^{4/5} \quad (6)$$

$$A(X) = (3/5) (PX^{-1/3})^{4/5} \quad (7)$$

$$Y(X) = (3/4) (PX^{-1/3})^{4/5} \quad (8)$$

Further, the mean (subscript  $m$ ) wave crest celerity  $c_{am}$  of the mean wave amplitude  $a_m$  is [4]

$$c_{am}/(gh)^{1/2} = (1 + 2(a_m/h)^2)^{1/2} \quad (9)$$

### 2.3. Experimental Setup and Procedure

For the present experiments with mesh-packed slides the identical wave channel was used as for these involving free granular material. The instrumentation consisted of six Capacitance Wave Gauges (CWG) (Figure 2). The slide impact velocity  $V_s$  and the slide thickness  $s$  were measured by laser distance sensors mounted perpendicularly to the slide plane. In contrast to the previous experiments,  $V_s$  of the mesh-packed slides was not determined as a slide centroid velocity, but as the velocity of the slide front under dry conditions, given that the loose mesh bag does not allow for a correct capturing of the slide profile.

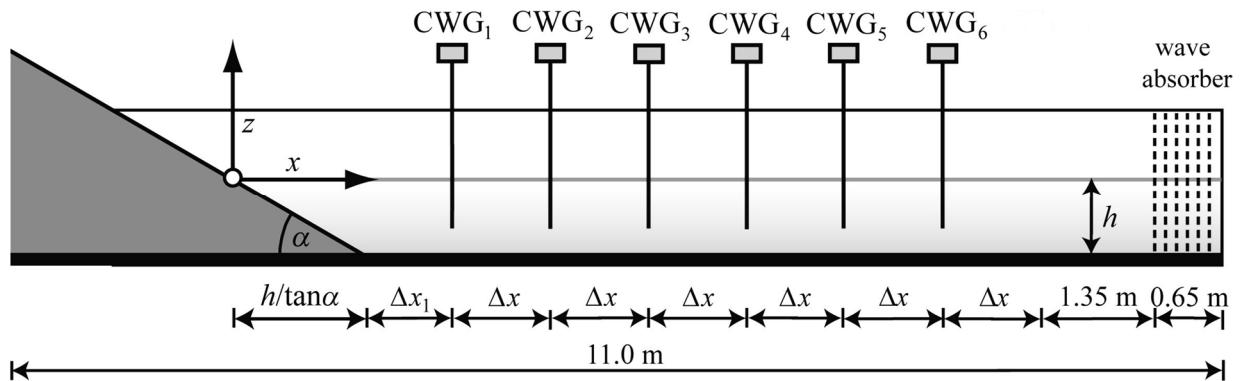


**Figure 2.** Capacitance Wave Gauge (CWG)<sub>1–6</sub> positions with  $\Delta x_1 = 0.71$  m and  $\Delta x = 1.00$  m for  $\alpha = 30^\circ$ ;  $\Delta x_1 = 1.13$  m and  $\Delta x = 1.00$  m for  $\alpha = 45^\circ$ ;  $\Delta x_1 = 1.27$  m and  $\Delta x = 1.06$  m for  $\alpha = 60^\circ$  (adapted from Heller [4], with permission from VAW).

**Table 1.** Overview of experimental parameters and dimensionless quantities.

Parameter	Free Granular Slides [4]	Mesh-Packed Slides
$h$ [m]	0.15, 0.20, 0.30, 0.45, 0.60, 0.675	0.20, 0.30, 0.40
$s$ [m]	0.05–0.249	0.062–0.145
$V_s$ [m/s]	2.06–8.77	1.2–9.2
$m_s$ [kg]	10.09–113.30	19.5–20.1
$\alpha$ [°]	30, 45, 60	30, 45, 60
$F$ [-]	0.86–6.83	0.70–5.36
$S$ [-]	0.09–1.64	0.16–0.65
$M$ [-]	0.11–10.02	0.24–1.01
$P$ [-]	0.17–8.13	0.26–2.78

The granular slide material used for the mesh-packed experiments corresponded to that used by Heller [4]. It has a grain (subscript  $g$ ) diameter of  $d_g = 8$  mm and a grain density of  $\rho_g = 2,429$  kg/m<sup>3</sup>. The granular material is loosely packed into mesh bags made of sifting media (SEFAR NYTAL® PA-38GG-500, Sefar AG, Heiden, Switzerland) with a mesh opening of 500  $\mu$ m and a porosity of 47%. The bags were accelerated with the pneumatic landslide generator [18]. The main parameters and dimensionless quantities of the mesh-packed slides considered herein are compared with these of the free granular slides in Table 1. The total number of mesh-packed experiments evaluated is 42.

### 3. Results and Discussion

#### 3.1. Slide Impact and Wave Generation Process

In Figure 3 the slide impact and wave generation processes are documented by means of high-speed photography at various times for slide impact angles of  $\alpha = 30^\circ$  and  $\alpha = 60^\circ$ . Free granular slides are affected by compaction and strong deformation processes during the impact onto the still water and the underwater movement to the channel bottom [3]. The mesh-packed slides are both bended and lifted upwards after impacting the water body, depending on the slide impact angle  $\alpha$ . For  $\alpha = 30^\circ$  these effects are larger than for  $\alpha = 60^\circ$ . These effects significantly increase the slide thickness  $s$  resembling the mechanisms of compaction and deformation of free granular slides. Also the process of flow separation and the formation of an impact crater along with air entrainment are observed in both cases.

#### 3.2. Maximum Wave Amplitude and Height

The relative maximum wave amplitude  $A_M$  and wave height  $Y_M$  of waves generated with mesh-packed slides versus the impulse product parameter  $P$  including Equations (5) and (6) are shown in Figure 4. The maxima are recorded independently from their position within the wave train and along their propagation distance. In most wave trains the wave maxima were observed at the first wave crest and were fully developed at CWG<sub>1</sub>. The data of both wave maxima predominantly scatter within  $\pm 30\%$  of Equations (5) and (6), as do these for free granular slides. A concentrated undercut of the  $-30\%$  curve for  $P \leq 1$  is also detected in the corresponding plots of Heller [4]. The coefficients of determination are  $R^2 = 0.82$  and  $R^2 = 0.85$  for maximum wave amplitude and height, respectively, compared to  $R^2 = 0.89$  and  $R^2 = 0.85$  for the 434 free granular slide experiments [4].

Note the effect of the slide impact angle  $\alpha$  on the relative maximum wave amplitude  $A_M$  and height  $Y_M$ . For  $\alpha = 60^\circ$  the maxima are predominantly scattered within the area between the curves of Equations (5) and (6) and their corresponding  $-30\%$  curves; at  $\alpha = 45^\circ$  the wave maxima are narrowly scattered along Equations (5) and (6), while the maxima of  $\alpha = 30^\circ$  are located in the upper half above the equations up to the  $+30\%$  curves. In summary, a good overall reproducibility of maximum impulse wave amplitudes and heights results by using mesh-packed slides.

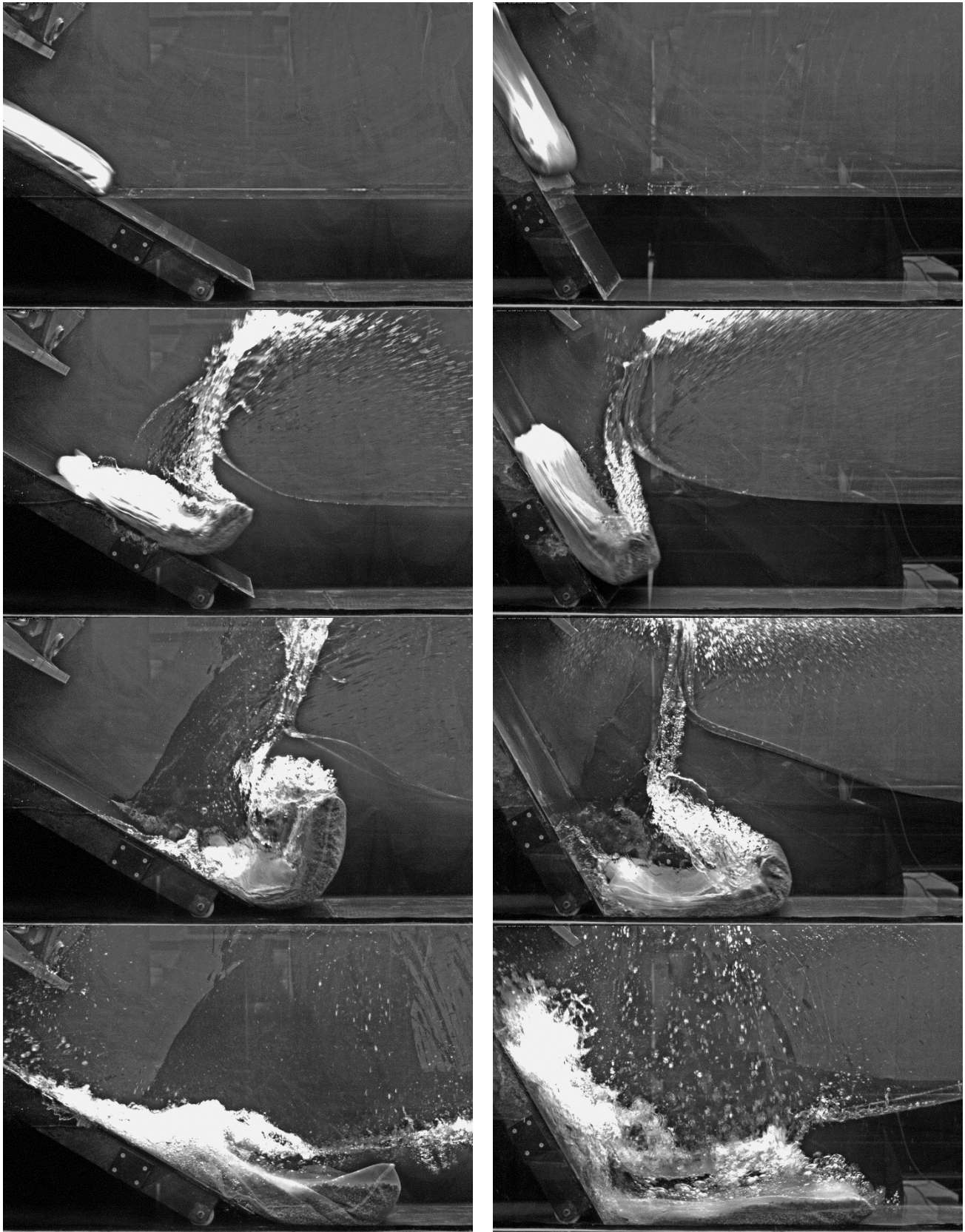


**Figure 3.** Photographs at various stages of wave generation process with mesh-packed slides. Left column:  $\alpha = 30^\circ$  with  $F = 2.27$ ,  $S = 0.23$ ,  $M = 0.45$ , and  $P = 0.84$  at  $t = 0.00, 0.14, 0.34$ , and  $0.90$  s. Right column:  $\alpha = 60^\circ$  with  $F = 3.03$ ,  $S = 0.21$ ,  $M = 0.45$ , and  $P = 0.90$ , at  $t = 0.00, 0.11, 0.31$ , and  $0.76$  s.

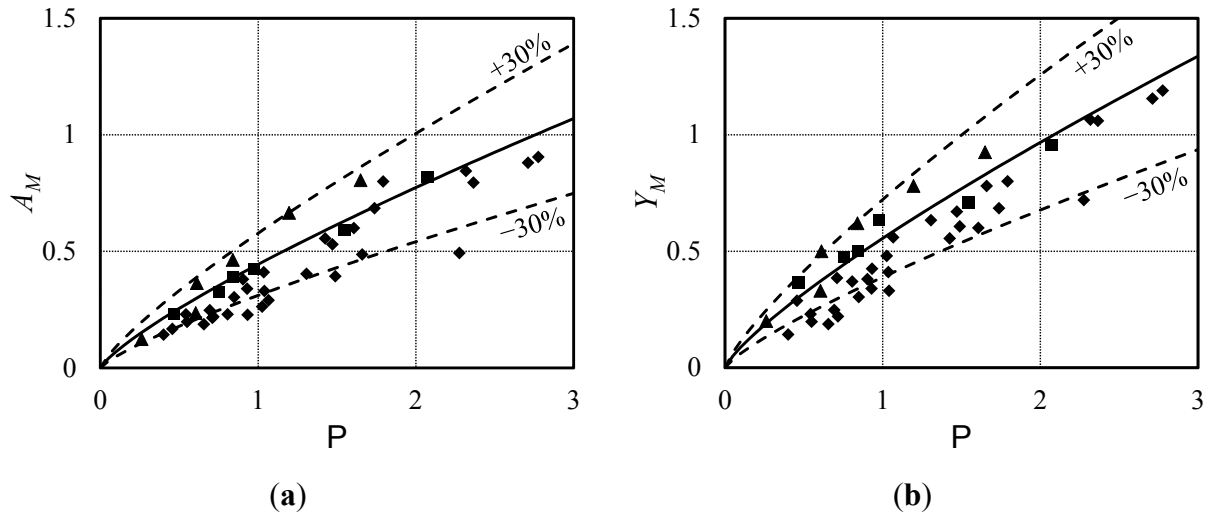


**Figure 4.** Waves generated by mesh-packed slides (a) relative maximum wave amplitude  $A_M(P)$  with (—) Equation (5); (b) wave height  $Y_M(P)$ , with (—) Equation (6) for ( $\blacktriangle$ )  $\alpha = 30^\circ$ , ( $\blacksquare$ )  $\alpha = 45^\circ$ , ( $\blacklozenge$ )  $\alpha = 60^\circ$ .

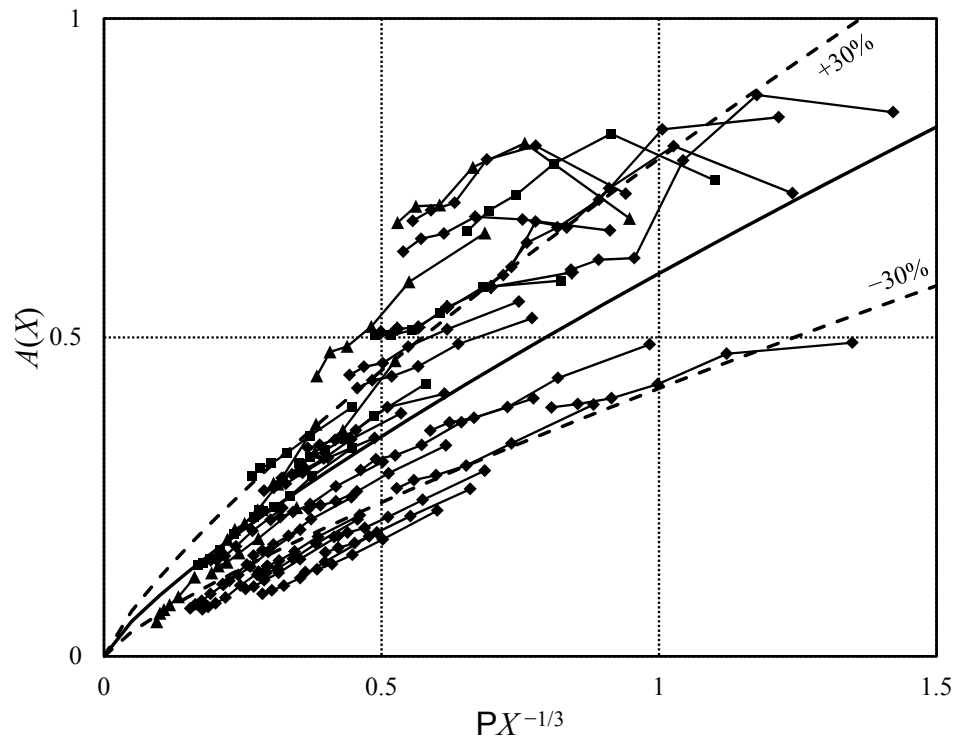
### 3.3. Wave Amplitude and Height Decay

To evaluate the wave amplitude and height decays, only the first wave crest was considered. This applies also to wave trains, where these maxima occur at the second wave crest. The relative wave amplitude  $A(X)$  and height  $Y(X)$  decays generated with mesh-packed slides versus  $PX^{-1/3}$  as well as the Equations (7) and (8) are shown in Figure 5, from where good overall agreement results. In contrast to the maxima of wave amplitude and height, no immediate effects of the slide impact angle  $\alpha$  result. For wave trains with  $PX^{-1/3} \leq 0.75$  at  $X_{CWG1}$  an increase in wave amplitude and height is observed. These wave trains developed their maxima at  $CWG_2$ . An increased undercut of the  $-30\%$  curve of Equation (7) of  $A(X)$  for  $PX^{-1/3} \leq 1$  applies also to the data of Heller [4]. This statement is valid for the data exceeding the  $+30\%$  curves of  $A(X)$  as well as  $Y(X)$  for  $0.5 \leq PX^{-1/3} \leq 1$ . Despite the values of wave amplitude and height decay that undercut and exceed the  $\pm 30\%$  curves of Equations (7) and (8) in certain ranges of  $PX^{-1/3}$ , they reproduce the results of free granular slides well. The coefficients of determination are  $R^2 = 0.71$  and  $R^2 = 0.78$  for wave amplitude and height decay, respectively, compared to  $R^2 = 0.83$  and  $R^2 = 0.84$  for the 434 free granular slide experiments [4].

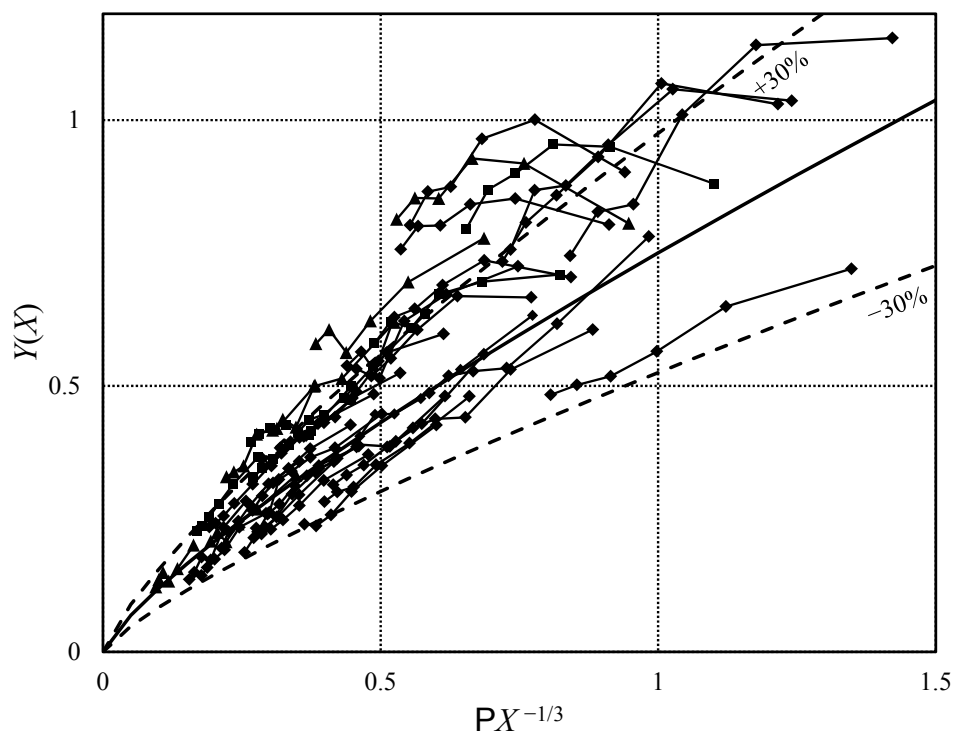
### 3.4. Wave Crest Celerity

The wave crest celerity was evaluated by averaging the wave amplitudes of the first crests of  $CWG_1$  to  $CWG_6$  to a mean wave amplitude  $a_m$ . By accounting for the runtime of the first wave crest between  $CWG_1$  to  $CWG_6$  the mean wave crest celerity  $c_{am}$  was determined in analogy to [4]. The relative celerity  $c_{am}/(gh)^{1/2}$  of waves generated with mesh-packed slides shown in Figure 6 lies within the experimental scatter of free granular material and reproduces Equation (9) well. The coefficient of determination is  $R^2 = 0.95$ , compared to  $R^2 = 0.91$  for the 434 free granular slide experiments [4].





(a)



(b)

**Figure 5.** Mesh-packed slides (a) relative wave amplitude decay  $A(X)$  with (—) Equation (7); (b) relative wave height decay  $Y(X)$  with (—) Equation (8) versus  $PX^{-1/3}$  for  $\alpha = 30^\circ$  ( $\blacktriangle$ ),  $\alpha = 45^\circ$  ( $\blacksquare$ ),  $\alpha = 60^\circ$  ( $\blacklozenge$ ).

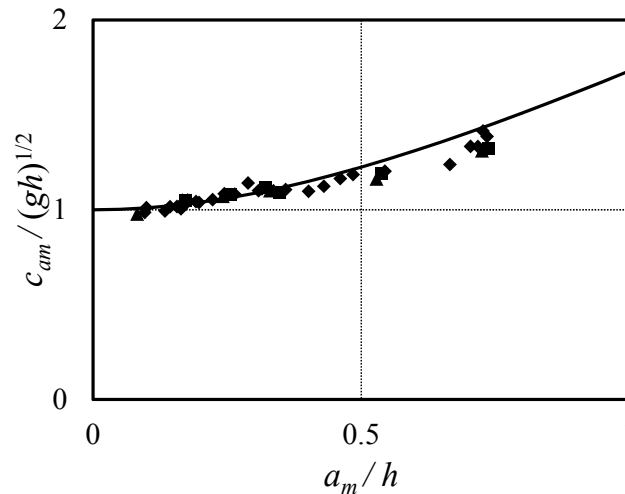


**Figure 6.** Waves generated by mesh-packed slides, mean relative wave crest celerity  $c_{am}/(gh)^{1/2}$  versus mean relative wave amplitude  $a_m/h$  for ( $\blacktriangle$ )  $\alpha = 30^\circ$ , ( $\blacksquare$ )  $\alpha = 45^\circ$ , ( $\blacklozenge$ )  $\alpha = 60^\circ$ , (—) Equation (9).

#### 4. Conclusions

This research explores the question whether impulse waves can be generated by mesh-packed slides as an alternative to free granular slides mainly in view of experimental effort and reduction of test preparation. Therefore, the prominent wave features induced by mesh-packed slides were investigated in a 2D wave channel. The impulse waves generated were analyzed regarding their main characteristics, including the maximum wave amplitude and height, the distance related decay, and the wave crest celerity. These features were compared with the previously established empirical equations derived from experiments involving free granular material to assess their reproducibility. The main findings are:

- The impulse product parameter  $P$  describes adequately both waves generated by mesh-packed and free granular slides;
- Waves generated by mesh-packed slides follow a  $\pm 30\%$  scatter around the equations derived from experiments with free granular material. This scatter applies equally to free granular slides;
- For small values of  $P$ , the present data may undercut the  $-30\%$  range. This behavior applies also for the corresponding ranges of free granular slides; and
- For values of  $PX^{-1/3}$  ranging between 0.5 and 1, the present data may exceed the  $+30\%$  range, similar as for free granular slides.

The present experiments evidence that mesh-packed slides suit for model experimentation of landslide-generated impulse waves which are physically similar regarding selected wave parameters to these generated with free granular material. This implies a substantial improvement of efficiency for the standard test procedure and is especially beneficial for future experiments in a wave basin.

#### Acknowledgments

This work was supported by the Swiss National Science Foundation (Project No 200021-143657/1).

## Author Contributions

The experiments were designed by WHH and FME. The experiments and the data analysis were conducted by FME. The article was written by FME and improved by WHH.

## Conflicts of Interest

The authors declare no conflict of interest.

## References

1. Heller, V.; Hager, W.H.; Minor, H.-E. Landslide generated impulse waves in reservoirs: Basics and computation. In *VAW-Mitteilung 211*; Minor, H.-E., Ed.; ETH Zurich: Zürich, Switzerland, 2009.
2. Heller, V.; Spinneken, J. Improved landslide-tsunami prediction: Effects of block model parameters and slide model. *J. Geophys. Res.-Oceans* **2013**, *118*, 1489–1507; doi:10.1002/jgrc.20099.
3. Fritz, H.M. Initial phase of landslide generated impulse waves. In *VAW-Mitteilung 178*; Minor, H.-E., Ed.; ETH Zurich: Zürich, Switzerland, 2002.
4. Heller, V. Landslide generated impulse waves: Prediction of near field characteristics. In *VAW-Mitteilung 204*; Minor, H.-E., Ed.; ETH Zurich: Zürich, Switzerland, 2008.
5. Mohammed, F.; Fritz, H.M. Physical modeling of tsunamis generated by three-dimensional deformable granular landslides. *J. Geophys. Res.* **2012**, *117*, C11015; doi:10.1029/2011JC007850.
6. Viroulet, S.; Sauret, A.; Kimmoun, O. Tsunami generated by a granular collapse down a rough inclined plane. *Europhys. Lett.* **2014**, *105*, 34004; doi:10.1209/0295-5075/105/34004.
7. Di Risio, M.; De Girolamo, P.; Bellotti, G.; Panizzo, A.; Aristodemo, F.; Molfetta, M.G.; Petrillo, A.F. Landslide-generated tsunamis runup at the coast of a conical island: New physical model experiments. *J. Geophys. Res.* **2009**, *114*, C01009; doi:10.1029/2008JC004858.
8. Kamphuis, J.W.; Bowering, R.J. Impulse waves generated by landslides. In Proceedings of the 12th Coastal Engineering Conference, Washington, DC, USA, 1970; pp. 575–588; doi:10.9753/icce.v12.%25p.
9. Noda, E. Water waves generated by landslides. *J. Waterway Div.-ASCE* **1970**, *96*, 835–855.
10. Panizzo, A.; de Girolamo, P.; Petaccia, A. Forecasting impulse waves generated by subaerial landslides. *J. Geophys. Res.* **2005**, *110*, C12025; doi:10.1029/2004JC002778.
11. Sælevik, G.; Jensen, A.; Pedersen, G. Experimental investigation of impact generated tsunami; related to a potential rock slide, Western Norway. *Coast. Eng.* **2009**, *56*, 897–906; doi:10.1016/j.coastaleng.2009.04.007.
12. Viroulet, S.; Cébron, D.; Kimmoun, O.; Kharif, C. Shallow water waves generated by subaerial solid landslides. *Geophys. J. Int.* **2013**, *193*, 747–762; doi:10.1093/gji/ggs133.
13. Ataie-Ashtiani, B.; Nik-Khah, A. Impulsive waves caused by subaerial landslides. *Environ. Fluid Mech.* **2008**, *8*, 263–280; doi:10.1007/s10652-008-074-7.
14. Zweifel, A. Impulswellen: Effekte der Rutschdichte und der Wassertiefe (Impulse waves: Effects of slide density and water depth). In *VAW-Mitteilung 186*; Minor, H.-E., Ed.; ETH Zurich: Zürich, Switzerland, 2004.

15. Slingerland, R.L.; Voight, B. Evaluating hazard of landslide-induced water waves. *J. Waterw. Port C. Div.* **1982**, *108*, 504–512.
16. Davidson, D.D.; Whalin, R.W. *Potential landslide-generated water waves, Libby Dam and Lake Koocanusa, Montana*; Technical Report H-74–15; Waterway Experiment Station, U.S. Army Corps of Engineers: Vicksburg, MO, USA, 1974.
17. Heller, V.; Hager, W.H. Impulse product parameter in landslide generated impulse waves. *J. Waterw. Port C-ASCE* **2010**, *136*, 145–155; doi:10.1061/(ASCE)WW.1943-5460.0000037.
18. Fritz, H.M.; Moser, P. Pneumatic landslide generator. *Int. J. Fluid Power* **2003**, *4*, 49–57; doi:10.1080/14399776.2003.10781155.

© 2015 by the authors; licensee MDPI, Basel, Switzerland. This article is an open access article distributed under the terms and conditions of the Creative Commons Attribution license (<http://creativecommons.org/licenses/by/4.0/>).